Atmospheric
Chemistry
and Physics
Discussions

Two new sources of reactive gaseous mercury in the free troposphere

H. Timonen[1,2], J. L. Ambrose[1], and D. A. Jaffe[1,3]

[1]Science and Technology Program, University of Washington-Bothell, Bothell, WA, USA
[2]Air Quality Research, Finnish Meteorological Institute, Helsinki, Finland
[3]Department of Atmospheric Sciences, University of Washington, Seattle, WA, USA

Correspondence to: H. Timonen (hilkka.timonen@fmi.fi)

ACPD

12, 29203–29233, 2012

Two new sources of reactive gaseous mercury in the free troposphere

H. Timonen et al.

Title Page

Abstract	Introduction
Conclusions	References
Tables	Figures

|◄ | ►|
◄ | ►

Back | Close

Full Screen / Esc

Printer-friendly Version

Interactive Discussion

Abstract

Mercury (Hg) is a neurotoxin that bioaccumulates in the food chain. Mercury is emitted to the atmosphere primarily in its elemental form, which has a long lifetime allowing global transport. It is known that atmospheric oxidation of gaseous elemental mercury
5 (GEM) generates reactive gaseous mercury (RGM) which plays an important role in the atmospheric mercury cycle by enhancing the rate of mercury deposition to ecosystems. However, the primary GEM oxidants, and the sources and chemical composition of RGM are poorly known. Using speciated mercury measurements conducted at the Mt. Bachelor Observatory since 2005 we present two previously unidentified
10 sources of RGM to the free troposphere (FT). Firstly, we observed elevated RGM concentrations, large RGM/GEM-ratios, and anti-correlation between RGM and GEM during Asian long-rang transport events, demonstrating that RGM is formed from GEM by in-situ oxidation in some anthropogenic pollution plumes in the FT. During the Asian pollution events the measured RGM/GEM-ratios reached peak values, up to ∼ 0.20,
15 which are significantly larger than ratios typically measured (RGM/GEM < 0.05) in the Asian source region. Secondly, we observed very high RGM levels – the highest reported in the FT – in clean air masses that were processed upwind of Mt. Bachelor Observatory over the Pacific Ocean. The high RGM concentrations (up to 700 pg m^{-3}), high RGM/GEM-ratios (up to 1), and very low ozone levels during these events pro-
20 vide the first observational evidence indicating significant GEM oxidation in the lower FT. The identification of these processes changes our conceptual understanding of the formation and distribution of oxidized Hg in the global atmosphere.

1 Introduction

During the last decade the measurements of atmospheric mercury (Hg) have devel-
25 oped substantially. Speciated Hg measurements (including gaseous elemental mercury (GEM), reactive gaseous mercury (RGM), and particle bound mercury (PBM);

Landis et al., 2002) are providing important information about mercury sources, transformation and subsequent deposition (e.g. Talbot et al., 2008; Peterson et al., 2009; Gustin and Jaffe, 2010; Sprovieri et al., 2010). Mercury is mainly emitted to the atmosphere in its elemental form, which has a long lifetime allowing global transport (Jaffe et al., 2005; NRC, 2010). Atmospheric oxidation of GEM generates gas– and particle phase oxidized Hg compounds (thought to be primarily inorganic Hg(II) species) that deposit quickly as they are more reactive, more water-soluble, and less volatile (Schroeder and Munthe, 1998; Lin and Pehkonen, 1999; Holmes et al., 2009; NRC, 2010). The spatial distribution of mercury deposition in many instances might thus depend more on atmospheric conditions (e.g. wind direction, oxidant concentrations, temperature) than on proximity to mercury sources (Chand et al., 2008; Sprovieri et al., 2010; Holmes et al., 2010; Rothenberg et al., 2010).

Information on transport and transformation of Hg in the free troposphere (FT) is scarce due to a poor understanding of sources of RGM and lack of long-term measurements at high elevations. The few Hg observations above the boundary layer (BL) demonstrate that the upper troposphere/lower stratosphere (UT/LS) is depleted in GEM and enriched in reactive mercury (RM = RGM + PBM; Murphy et al., 2006; Swartzendruber et al., 2006, 2008; Talbot et al., 2007, 2008; Lyman and Jaffe, 2011). Oxidation of GEM in the stratosphere (coupled with stratosphere to troposphere transport) is the only known source of RGM above the BL (Murphy et al., 2006; Swartzendruber et al., 2006; Lyman and Jaffe, 2011). However, based on previous studies and calculations this source accounts for only a small fraction of tropospheric RGM (Lyman and Jaffe, 2011). Although halogen species might also play a role in GEM oxidation in the FT, the existing observations and model studies have not clearly proven this. Therefore, the sources and RGM formation mechanisms in the bulk of the global atmosphere remain poorly characterized. Using observations of speciated mercury (GEM, RGM, and PBM), submicron aerosol scattering (σ_{sp}), trace gases (ozone, O_3; carbon monoxide, CO) and meteorology from the Mt. Bachelor Observatory (MBO), we describe in this paper two new sources of RGM in the FT.

2 Experimental

2.1 Mt. Bachelor observatory

The Mount Bachelor observatory (MBO) is located on the summit of Mt. Bachelor in Central Oregon, USA (43.981° N, 121.691° W, 2.7 km a.s.l.). The site is approximately 180 km east of the Pacific coast. Past work has demonstrated that MBO is suitable for observing FT airmasses with minimal influence form North American anthropogenic emissions (Jaffe et al., 2005; Weiss-Penzias et al., 2006; Ambrose et al., 2011; Fischer et al., 2011).

2.2 Measurements

Speciated Hg (gaseous elemental mercury (GEM), reactive gaseous mercury (RGM), and particle bound mercury (PBM)) measurements have been conducted at MBO since 2005 using a Tekran 2537A Hg vapor analyzer and a Tekran 1130/1135 Hg speciation system. A detailed description of the sampling system can be found in Swartzendruber et al. (2006). Briefly, a Teflon-coated aluminum (Al) cyclone inlet (URG Corp.), coupled to a Teflon-coated Al high-volume inlet (URG), was used for sampling. The flow through the high-volume inlet was maintained between 50 and 100 std l min^{-1} (standard pressure of 1.01 bar and temperature of 273.15 K). The speciation system sampled 7.5 std l min^{-1} from the high-volume inlet. A KCl coated annular denuder was used to collect RGM and a quartz fiber filter was used to collect PBM. Downstream of the speciation system the Tekran 2537A sampled an additional 0.65 std l min^{-1} from the airstream and measured GEM at 5 min intervals. The total flow through the cyclone inlet yielded a particle size cut of 2.5 μm. To improve the RM detection limit, RGM and PBM samples were collected for 3 h prior to analysis. During the RGM and PBM analysis cycle (60 min) GEM was not measured. The Hg instruments were calibrated with the elemental mercury (Hg^0) permeation source internal to the Tekran 2537A. The emission rate of the permeation source was verified by injections of Hg^0 from a Tekran

2505 saturated Hg^0 vapor source, using a gas-tight microliter syringe (Hamilton). There are uncertainties about the calibration and interferences in the Tekran RGM measurements (Lyman et al., 2010; Gustin et al., 2012; Ambrose et al., 2012). Nonetheless, until these issues can be definitively resolved, we assume the Tekran RGM measurements
5 represent all oxidized forms of Hg in the atmosphere, similar to most researchers.

Aerosol measurements conducted at MBO since 2004 are described in detail by Fischer et al. (2011). Briefly, a Radiance Research nephelometer (M903) was used to measure scattering coefficient at mid-visible wavelength (530 nm). Aerosol concentrations were estimated from the scattering (σ_{sp}) coefficient using a dry mass scattering
10 efficiency value of 3.0 (Hand and Malm, 2007). The cutoff diameter was changed from 1 µm to 2.5 µm at the beginning of 2010. The rotating drum impactor, developed at the University of California, (Raabe et al., 1988; Perry et al., 2004) was used to measure the elemental composition (Na, Mg, Al, Si, P, S, Cl, K, Ca, Ti, V, Cr, Mn, Fe, Ni, Zn, Ga, As, Se, Br, Rb, Sr, Y, Zr, Mo, Pb) of ambient aerosols at the following size
15 classes (D_a) > 5.0, 5.0–2.5, 2.5–1.1, 1.1–0.75, 0.75–0.56, 0.56–0.34, 0.34–0.26, and 0.26–0.09 µm. The elemental composition of samples collected to mylar- substrates was analyzed using a synchrotron Xray fluorescence (SXRF) technique (Haller and Knochel, 1996; Perry et al., 2004). The blank values were determined by analyzing the blank portions of both ends of the used mylar substrates.
20 Measurements of CO, O_3 and submicron aerosol scattering (σ_{sp}) are described in Ambrose et al. (2011). Briefly, Ozone and CO concentrations were measured with Dasibi 1008-RS and TECO 48C Trace level Enhanced CO analyzers (Weiss-Penzias et al., 2006; Jaffe et al., 2005; Weiss-Penzias et al., 2006, 2007). Vaisala PTB101B transmitter was used to measure pressure and Campbell Scientific HMP45C probe
25 was used to monitor the ambient temperature (T) and relative humidity (RH).

2.3 Back trajectory modeling

We calculated 10-day airmass backward trajectories for each high RGM event to establish the transport history of the associated air masses. Trajectories were calculated using the NOAA Hybrid Single-Particle Lagrangian Integrated Trajectory model (HYS-PLIT, v4.9, Draxler and Rolph, 2012) and global meteorological data from the Global Data Assimilation System (GDAS) archive, having a horizontal resolution of $1° \times 1°$, 3 h time resolution, and a vertical resolution of 23 pressure surfaces between 1000 and 20 hPa. During events trajectories were initialized from the summit of MBO for the hours when the highest RGM/GEM-ratios were observed.

2.4 Statistical analysis

Due to error in both x and y variables and the relatively small number of RGM observations during each event, correlations between measured compounds were calculated using the Williamson-York Iterative Bivariate Fit method (Cantrell et al., 2008).

3 Results

RGM measurements in the FT are scarce and thus the identification of mercury sources and characterization of the global mercury cycle has been a challenge. Transport of RGM from the stratosphere (type 1. UTLS event) is the only known source of RGM above the BL (Murphy et al., 2006; Swartzendruber et al., 2006; Lyman and Jaffe, 2011). During UT/LS type 1 events an increase in RGM and ozone concentrations and a clear correlation between RGM and ozone is typically observed (Swartzendruber et al., 2006). Also, during these events, a clear decrease in GEM, CO and aerosol concentrations is observed, coinciding with the RGM and O_3 enhancements (Swartzendruber et al., 2006). Using mercury (GEM, RGM, PBM), aerosol (scattering and elemental composition) and trace gas (CO, O_3) measurements conducted at MBO since 2005 we present here two previously unidentified sources of RGM to the FT.

Full Screen / Esc

Printer-friendly Version

Interactive Discussion

Figure 1 shows a conceptual model of the three types of RGM sources to the lower FT (1, UT/LS; 2, Asian long-range transport (ALRT); 3, marine boundary layer (MBL)) observed at MBO. Type 1 (UT/LS) events were identified previously by Swartzendruber et al. (2006) and will not be discussed here. Type 2 ALRT and type 3 MBL events are described in Sects. 3.1 and 3.2.

3.1 Anthropogenic RGM events (type 2)

First, we present evidence for in-situ oxidation of GEM to RGM (yielding RGM/GEM-ratios up to 0.18) in anthropogenic pollution plumes that were transported from Asia to the free troposphere over the US Pacific Northwest (source type 2). This is important because oxidation of GEM in long-range transported pollution plumes in the FT has not been observed previously (Jaffe et al., 2005; Swartzendruber et al., 2006; Faïn et al., 2009). Previous studies conducted in urban areas have shown that point source emissions affect the GEM and RGM concentrations in downwind areas (Lynam and Keeler, 2005; Rothenberg et al., 2009). However, these studies were not able to identify in-situ production of RGM. During springtime, meteorological conditions are favorable for transpacific transport and Asian pollution plumes are repeatedly observed at MBO (Jaffe et al., 2005; Weiss-Penzias et al., 2006; Ambrose et al., 2011). Increasing anthropogenic Hg emissions in developing Asian countries (Pacyna et al., 2010; Fu et al., 2012), coupled with formation of RGM during long-range transport will enhance Hg deposition downwind in North America.

We present three clear ALRT events (Fig. 2, Table 1) with total Hg (THg = GEM + RGM + PBM) and RGM concentrations substantially elevated above typical background FT levels. Atmospheric concentrations of Hg species and trace gases, aerosol scattering values, and correlations between main components are shown for each event in Table 1. During ALRT events airmass back trajectories show direct transport from Asia in ≤ 10 days (Fig. 3). In addition, the THg/CO enhancement ratios (on average $0.0069\,\mathrm{ng\,m^{-3}\,ppbv^{-1}}$; Fig. 4) were consistent with the ratios measured previously in Asian plumes (Jaffe et al., 2005; Weiss-Penzias et al., 2007). Furthermore, aerosol

scattering (20–48 Mm^{-1}), CO (162–200 ppbv), and O$_3$ (72–80 ppbv) were enhanced to levels typically measured in Asian pollution plumes at MBO (Jaffe et al., 2005; Weiss-Penzias et al., 2007; Ambrose et al., 2011) (Table 1). Also, the O$_3$/CO correlation slopes (unitless) for these events (0.1–0.3) were in the range of values that are typically seen in Asian pollution plumes with no UT/LS influence (Price et al., 2004). During ALRT events PBM concentrations were low (< 15 pg m^{-3}), amounting to < 15 % of reactive mercury (see Sect. 3.3 for more information).

During ALRT events RGM was correlated with the anthropogenic pollution tracers CO, σ_{sp} and/or O$_3$ (Table 1), indicating that they have a common origin. Furthermore, RGM and GEM were anti-correlated in the ALRT plumes. The RGM enhancements corresponded with GEM depletions of 0.2–0.4 ng m^{-3} (Fig. 2). This indicates that we are seeing the effects of conversion of GEM to RGM in-situ, rather than primary Asian RGM. Depletion of GEM in anthropogenic pollution plumes has only been seen previously in the BL (Weiss-Penzias et al., 2003; Lynam and Keeler, 2005). Several studies have measured RGM and GEM concentrations in China and in Asian pollution plumes in the Western Pacific BL (Jaffe et al., 2005; Chand et al., 2008; Fu et al., 2012). The RGM/GEM-ratios observed were typically below 0.03. In contrast, for the three ALRT events presented in this paper the peak RGM/GEM-ratio was between 0.15 and 0.18, showing that the measured RGM is a significant fraction of THg (Table 1, Fig. 2). Previous studies have shown that for primary RGM emissions a positive correlation between RGM and GEM is typically observed, whereas for in-situ oxidation an anti-correlation between RGM and GEM is expected (Swartzendruber et al., 2006; Sillman et al., 2007). The anti-correlation between RGM and GEM (Table 1, Fig. 5) and elevated RGM/GEM-ratios in ALRT plumes observed at MBO, indicate that the source of RGM during these events was in-situ oxidation during FT transport. Previous studies have shown that the lifetime of RGM is longer in the FT than in the BL due to the absence of removal mechanisms (Munthe et al., 2003; Selin et al., 2007). Therefore, conditions in the FT are expected to be more favorable for accumulation and transport of secondary (e.g. photochemical) RGM.

3.2 Marine boundary layer events (type 3)

The second new RGM source we have identified (type 3; marine boundary layer) occurs in very clean air masses. The air mass back trajectories show that these air masses had circled above the Pacific Ocean for at least 10 days prior to arriving at
5   MBO (Figs. 1 and 6). Here we present four clear MBL events (Fig. 7, Table 1). During MBL events a simultaneous increase in RGM and decrease in CO, aerosol scattering, and O_3 was observed. The low CO and aerosol scattering values (Fig. 7, Table 1) measured during this time period suggest minimal influence from anthropogenic emissions or from biomass burning (Munthe et al., 2003; Weiss-Penzias et al., 2007). The O_3 and
10 water vapor mixing ratios ($\sim$ 30–45 ppbv and 3–4 g kg^{-1}, respectively) during the event do not indicate transport from the UT/LS; rather, the composition of these air masses is more consistent with an influence from the clean sub-tropical MBL.

The RGM concentrations observed during MBL events were very high (200–700 pg m^{-3}) compared to anthropogenic pollution plumes (200–300 pg m^{-3}) (Table 1).
15 Such high RGM levels have been measured in the BL near emission sources and locations with high concentrations of oxidants (e.g. those encountered at the Dead Sea; Obrist et al., 2010). However, such high levels have not been previously observed in the FT. Much lower THg concentrations were measured during MBL events (1.2–1.4 ng m^{-3}) when compared to anthropogenic pollution plumes (1.7–1.8 ng m^{-3}). As for
20 Type 2 events, PBM concentrations were low (< 12 pg m^{-3}), amounting to < 15 % of reactive mercury. A clear anti-correlation between RGM and GEM was observed during MBL events (Table 1, Fig. 7) indicating in-situ GEM oxidation. Furthermore, the large RGM/GEM-ratios (0.31–1.05, Table 1) demonstrate an efficient process for GEM oxidation and transport of RGM in the FT. It is notable that the large RGM enhancements in
25 these air masses far exceed those previously observed in UT/LS influenced air masses (Swartzendruber et al., 2006; Ambrose et al., 2011).

Aerosol chemical composition was measured with rotating DRUM impactors during the MBL event observed in May 2011. A small increase in aerosol sea salt (Na$^+$ and

Cl⁻) concentration was measured, further indicating that the air mass likely originated from the marine boundary layer. Sea salt aerosol may be an important sink for RGM in the MBL (Malcolm et al., 2009), thus explaining smaller ambient RGM concentrations observed in the studies conducted in marine regions (Laurier et al., 2003; Laurier and Mason, 2007).

3.3 Particle bound mercury (PBM)

Reactive mercury (RM) is defined as the sum of reactive gaseous mercury (RGM) and particle bound mercury (PBM). During the measurement period (2005–2012) the PBM concentrations were usually low (below $30\,\mathrm{pg\,m^{-3}}$) in the FT. Elevated PBM concentrations (30–$45\,\mathrm{pg\,m^{-3}}$) were mainly observed during biomass burning episodes (Finley et al., 2009), when the emissions clearly originated from the boundary layer. During RGM events described in this paper PBM concentrations were low ($< 15\,\mathrm{pg\,m^{-3}}$), amounting to less than 15 % of RM. The contribution of PBM is clearly lower than expected based on RM partitioning coefficients derived from measurements in the BL at low altitude sites (Rutter and Schauer, 2007b; Amos et al., 2012). However, previous studies have demonstrated that partitioning of RM (and other semivolatile species) between the gas and aerosol phase depends on conditions such as temperature (Rutter and Schauer, 2007b; Amos et al., 2012); aerosol concentration and composition (Rutter and Schauer, 2007a; Amos et al., 2012); and possibly also relative humidity (Pankow et al., 1994; Xiu et al., 2009; Kim et al., 2012). Furthermore, previous studies suggest that heterogeneous reactions at surfaces potentially play a key role in Hg chemistry (Subir et al., 2012). The conditions in the FT (e.g. dry air; low temperature and pressure; high solar radiation intensity; Jaffe et al., 2005; Weiss-Penzias et al., 2006), are substantially different than in the boundary layer; therefore, RM partitioning behavior likely also differs between the FT and BL. If partitioning of RM to PBM is enhanced in the presence of an aerosol aqueous phase, the lower relative humidity in the FT will likely favor partitioning of RM to RGM more so than in the BL. Also, due to below freezing temperatures in the free troposphere, it is likely that aerosol particles will

incorporate ice rather than liquid water. The interfacial chemistry of Hg on ice surfaces is poorly known (Subir et al., 2012), although it appears that the uptake of RGM to ice is less efficient than for liquid water (Sigler et al., 2009). We note that previous studies have also measured low PBM concentrations in the free troposphere (Murphy et al., 2006).

3.4 Oxidation mechanisms

Gaseous halogen species, in particular bromine atom (Br$^\bullet$), chlorine atom (Cl$^\bullet$), and bromine oxide (BrO$^\bullet$), may be important oxidants for GEM in the atmosphere (Swarzendruber et al., 2006; Holmes et al., 2009; 2010; Subir et al., 2011; Stephens et al., 2012; Tas et al., 2012). In addition, O$_3$ and hydroxyl radical (HO$^\bullet$) might also contribute to GEM oxidation, although the associated mechanisms are more uncertain than for halogen atoms (Holmes et al., 2010; Rutter et al., 2012; Subir et al., 2012). The three main sources of RGM observed at MBO represent contrasting air mass types: dry upper tropospheric air with high O$_3$ and RGM concentrations (type 1); aged Asian anthropogenic emissions with elevated Hg concentrations (type 2); and clean air with background Hg and a potential contribution from natural oceanic emissions (type 3). Thus, it is likely that the oxidation mechanisms converting GEM to RGM are different in each case. Production of RGM in type 1 events (Swarzendruber et al., 2006) is likely associated with Br$^\bullet$chemistry in the UT/LS region (Holmes et al., 2010).

The RGM concentrations during ALRT events (type 2) were clearly correlated with anthropogenic pollution tracers (CO or σ_{sp}) possibly indicating that the oxidant has an anthropogenic origin. The RGM associated with type 2 events could also be produced by halogens, but the mechanism is not clear. Previous studies have indicated that Cl$^\bullet$could be generated from the interaction of pollution plumes with chloride (Cl$^-$) containing aerosols (Lawler et al., 2009; Thornton et al., 2009). Oxidation via heterogeneous chemistry involving aerosol particles is also a possible mechanism (Subir et al., 2012), and would be consistent with the observed correlation between the RGM and aerosol concentrations.

Two new sources of reactive gaseous mercury in the free troposphere

H. Timonen et al.

For type 3 (MBL) events a clear anti-correlation between RGM and O_3 was observed, indicating that O_3 is not likely an oxidant. Also, as these events are only seen in clean air masses, it seems unlikely that the oxidant would have an anthropogenic origin. More likely, reactive halogen chemistry plays an important role in these events. For the type 3 events, we believe that Br radicals are the likely oxidants. This is supported by box model calculations (see Sect. 3.4.1) using estimated Br$^•$ mixing ratios for the MBL. In the marine boundary layer, RGM enhancements have been reported (Laurier and Mason, 2007; Chand et al., 2008; Holmes et al., 2009), but these never reached the levels we observed in the FT. A possible explanation for the very high RGM concentrations observed during MBL events at MBO is that RGM could accumulate on aqueous super-micron sea-salt aerosol in the MBL (Rutter and Schauer, 2007a; Malcolm et al., 2009), and then subsequently partition back to the gas phase when lofted to the lower FT. For instance, lower relative humidity in the FT, and subsequent evaporation of the aerosol aqueous phase, could also favor partitioning of water-soluble sea salt-bound PBM to RGM. Furthermore, low relative humidity in the FT would favor partitioning of halogens to the gas phase, due to evaporation of the aerosol aqueous phase and associated decrease in pH (Lawler et al., 2009, 2011).

3.4.1 Box model calculations for type 3 (MBL) events

Based on previous studies, gaseous halogen species, in particular Br$^•$, are assumed to be important GEM oxidants in the MBL (Hedgecock and Pirrone, 2004; Holmes et al., 2009, 2010; Subir et al., 2012). Therefore, we used box model calculations to estimate the potential contribution of Br$^•$ chemistry to RGM production during type 3 (MBL) events. Figure 8 shows simulated Br-initiated oxidation of Hg^0 by the reaction mechanism including reactions Eqs. (1)–(4) (with rate data from Goodsite et al., 2004; Donohue et al., 2006; Holmes et al., 2010) for conditions representative of the 11 May

Title Page

Abstract | Introduction

Conclusions | References

Tables | Figures

◄ | ►|

◄ | ►

Back | Close

Full Screen / Esc

Printer-friendly Version

Interactive Discussion

2011 high-RGM event.

$$Hg^0 + Br^\bullet \xrightarrow{M} HgBr \tag{1}$$

$$HgBr \xrightarrow{M} Hg^0 + Br^\bullet \tag{2}$$

$$HgBr + Br^\bullet \xrightarrow{M} HgBr_2 \tag{3}$$

$$HgBr + HO^\bullet \xrightarrow{M} HgBrOH \tag{4}$$

Conditions used in the simulations are summarized in Table 2 and correspond with the median pressure (896 hPa) and temperature (282 K) along 10-day HYSPLIT backward trajectories that were initiated from MBO (1375 m a.g.l. on the model grid) during the event. The trajectories were initiated at the mid-points of the 3-h RM samples corresponding with the highest measured RGM concentrations. (Note that trajectories for this event leave the boundary layer 3.75–5.25 days prior to arrival at MBO.)

For a 10 day reaction time, with mean $[Br^\bullet]$ and $[HO^\bullet] = 0.035$ pptv and 0.5 to 1.5×10^6 molecules cm^{-3}, respectively (here brackets denote mixing ratio or concentration), the modeled [RGM] (142–175 pg m^{-3}) accounts for 52–64 % of the peak level (275 pg m^{-3}) observed at MBO during the 11 May event (Fig. 8, Table 2). Our results indicate that, for reasonable $Br^\bullet$ and $HO^\bullet$ concentrations, a large fraction of the peak RGM measured can be explained by $Br^\bullet$ chemistry alone. We note that the initial value of [THg] in the simulations (1.19 ng m^{-3} – the concentration corresponding with the RGM peak) is quite low for the MBL and lower FT in the Northern Hemisphere (Lindberg et al., 2007; Ambrose et al., 2011). Therefore, the low measured value of [THg] at the center of the event is consistent with loss of a substantial quantity of RM upwind of MBO. An alternative model scenario aimed at reproducing [GEM], [RGM], and [THg] at the center of the event could include higher initial [THg] (with a value closer to the mean background of ~ 1.5–1.7 ng m^{-3}; Lindberg et al., 2007; Ambrose et al., 2011) and a pathway for RGM removal.

4   Conclusions

Mercury is an important global pollutant, with a complex atmospheric cycle. Current models provide a rough outline of the global budget, but the atmospheric chemistry is poorly understood. Due to observed differences in behavior (e.g. sources, gas-particle
5 partitioning, and concentration levels) of Hg species in the FT in comparison to the BL, studies in the FT are needed to fully understand the chemical cycle of Hg. Using long-term Hg observations at the Mt. Bachelor Observatory we have identified two new sources of RGM in the atmosphere, which suggest stronger coupling between BL emissions and FT oxidation than previously recognized. For both source types, Hg
10 and its oxidants (or oxidant precursors) are likely first lofted from the BL (Asia, or the Pacific MBL) to the FT. Subsequently, GEM is effectively converted to RGM in the FT on relatively short timescales (several days) during long-range transport to downwind regions. The RGM generated will eventually be entrained back to the BL (Lyman and Gustin, 2009; Weiss-Penzias et al., 2009), deposited and incorporated to biota. We
15 believe also that changes in RM gas-particle partitioning during transport could also contribute to the high observed RGM concentrations during MBL events. Results of this study offer new directions for process oriented studies of the atmospheric mercury cycle.

References

25 Ambrose, J. L., Reidmiller, D. R., and Jaffe, D. A.: Causes of high O_3 in the lower free troposphere over the Pacific Northwest as observed at the Mt. Bachelor Observatory, Atmos. Environ., 45, 5302–5315, doi:10.1016/j.atmosenv.2011.06.056, 2011.

Ambrose, J. L., Lyman, S. N., Huang, J., Gustin, M. S., and Jaffe, D. A.: Fast time resolution oxidized mercury measurements during the Reno Atmospheric Mercury Intercomparison Experiment (RAMIX), Environ. Sci. Technol., in review, 2012.

Amos, H. M., Jacob, D. J., Holmes, C. D., Fisher, J. A., Wang, Q., Yantosca, R. M., Corbitt, E. S., Galarneau, E., Rutter, A. P., Gustin, M. S., Steffen, A., Schauer, J. J., Graydon, J. A., Louis, V. L. St., Talbot, R. W., Edgerton, E. S., Zhang, Y., and Sunderland, E. M.: Gas-particle partitioning of atmospheric Hg(II) and its effect on global mercury deposition, Atmos. Chem. Phys., 12, 591–603, doi:10.5194/acp-12-591-2012, 2012.

Cantrell, C. A.: Technical Note: Review of methods for linear least-squares fitting of data and application to atmospheric chemistry problems, Atmos. Chem. Phys., 8, 5477–5487, doi:10.5194/acp-8-5477-2008, 2008.

Chand, D., Jaffe, D., Prestbo, E., Swartzendruber, P. C., Hafner, W., Weiss-Penzias, P., Kato, S., Takami, A., Hatakeyama, S., and Kajii, Y.: Reactive and particulate mercury in the Asian marine boundary layer, Atmos. Environ., 42, 7988–7996, 2008.

Donohoue, D., Bauer, D., Cossairt, B., and Hynes, A.: Temperature and pressure dependent rate coefficients for the reaction of Hg with Br and the reaction of Br with Br: a pulsed laser photolysispulsed laser induced fluorescence study, J. Phys. Chem. A., 110, 6623–6632, doi:10.1021/jp054688j, 2006.

Draxler, R. R. and Rolph, G. D.: HYSPLIT (HYbrid Single-Particle Lagrangian Integrated Trajectory) Model, access via NOAA ARL READY Website, available at: http://ready.arl.noaa.gov/HYSPLIT.php, NOAA Air Resources Laboratory, Silver Spring, MD, 2012.

Faïn, X., Obrist, D., Hallar, A. G., Mccubbin, I., and Rahn, T.: High levels of reactive gaseous mercury observed at a high elevation research laboratory in the Rocky Mountains, Atmos. Chem. Phys., 9, 8049–8060, doi:10.5194/acp-9-8049-2009, 2009.

Finley, B. D., Swartzendruber, P. C., and Jaffe, D. A.: Particulate mercury emissions in regional wildfire plumes observed at the Mount Bachelor Observatory, Atmos. Environ., 43, 6074–6083, 2009.

Fischer, E. V., Perry, K. D., and Jaffe, D. A.: Optical and chemical properties of aerosols transported to Mount Bachelor during spring 2010, J. Geophys. Res., 116, D18202, doi:10.1029/2011JD015932, 2011.

Fu, X., Feng, X., Sommar, J., and Wang, S. A.: review of studies on atmospheric mercury in China, Sci. Total Environ., 421–422, 73–81, 2012.

Two new sources of reactive gaseous mercury in the free troposphere

H. Timonen et al.

Goodsite, M., Plane, J., and Skov, H.: A theoretical study of the oxidation of Hg^0 to $HgBr_2$ in the troposphere, Environ. Sci. Technol., 38, 1772–1776, doi:10.1021/es034680s, 2004.

Gustin, M. and Jaffe, D.: Reducing the uncertainty in measurement and understanding of mercury in the atmosphere, Environ. Sci. Technol., 44, 2222–2227, doi:10.1021/es902736k, 2010.

Gustin, M. S., Huang, J., Miller, M. B., Finley, B. D., Call, K., Ambrose, J. L., Peterson, C., Lyman, S. N., Everhart, S., Bauer, D., Remeika, J., Hynes, A., Jaffe, D. A., Lindberg, S. E.: RAMIX – a step towards understanding mercury atmospheric chemistry and Tekran[®] observations, Environ. Sci. Technol., in review, 2012.

Haller, M. and Knochel, W.: X-ray fluorescence analysis using synchrotron radiation (SYXRF), J. Trace Microprobe Technol., 14, 461–488, 1996.

Hand, J. L. and Malm, W. C.: Review of aerosol mass scattering efficiencies from ground-based measurements since 1990, J. Geophys. Res., 112, D16203, doi:10.1029/2007JD008484, 2007.

Hedgecock, I. M. and Pirrone, N.: Chasing quicksilver: modeling the atmospheric lifetime of $Hg_{(g)}$ in the marine boundary layer at various latitudes, Environ. Sci. Technol., 38, 69–76, 2004.

Holmes, C. D., Jacob, D. J., Mason, R. P., and Jaffe, D. A.: Sources and deposition of reactive gaseous mercury in the marine atmosphere, Atmos. Environ., 43, 2278–2285, doi:10.1016/j.atmosenv.2009.01.051, 2009.

Holmes, C. D., Jacob, D. J., Corbitt, E. S., Mao, J., Yang, X., Talbot, R., and Slemr, F.: Global atmospheric model for mercury including oxidation by bromine atoms, Atmos. Chem. Phys., 10, 12037–12057, doi:10.5194/acp-10-12037-2010, 2010.

Jaffe, D. A., Prestbo, E., Swartzendruber, P., Weiss-Penzias, P., Kato, S., Takami, A., Hatakeyama, W., and Kajii, Y.: Export of atmospheric mercury from Asia, Atmos. Environ., 39, 3029–3038, 2005.

Kim, P.-R., Han, Y.-J., Holsen, T. M., and Yi, S.-M.: Atmospheric particulate mercury: concentrations and size distributions, Atmos. Environ., 61, 94–102, 2012.

Landis, M. S., Stevens, R. K., Schaedlich, F., and Prestbo, E. M.: Development and characterization of an annular denuder methodology for the measurement of divalent inorganic reactive gaseous mercury in ambient air, Environ. Sci. Tech., 36, 3000–3009, 2002.

Laurier, F. and Mason, R.: Mercury concentration and speciation in the coastal and open ocean boundary layer, J. Geophys. Res., 112, D06302, doi:10.1029/2006JD007320, 2007.

Laurier, F. J. G., Mason, R. P., Whalin, L., and Kato, S.: Reactive gaseous mercury formation in the North Pacific Ocean's marine boundary layer: a potential role of halogen chemistry, J. Geophys. Res., 108, D174529, doi:10.1029/2003JD003625, 2003.

Lawler, M. J., Finley, B. D., Keene, W. C., Pszenny, A. A. P., and Read, K. A.: Pollution-enhanced reactive chlorine chemistry in the Eastern tropical Atlantic boundary layer, Geophys. Res. Lett., 36, L08810, doi:10.1029/2008GL036666, 2009.

Lawler, M. J., Sander, R., Carpenter, L. J., Lee, J. D., von Glasow, R., Sommariva, R., and Saltzman, E. S.: HOCl and Cl_2 observations in marine air, Atmos. Chem. Phys., 11, 7617–7628, doi:10.5194/acp-11-7617-2011, 2011.

Lin, C.-J. and Pehkonen, S. O.: The chemistry of atmospheric mercury: a review, Atmos. Environ., 33, 2067–2079, 1999.

Lindberg, S. E., Bullock, R., Ebinghaus, R., Engstrom, D., Feng, X., Fitzgerald, W., Pirrone, N., Prestbo, E., and Seigneur, C.: A synthesis of progress and uncertainties in attributing the sources of mercury in deposition, Ambio, 36, 19–32, 2007.

Lyman, S. N. and Gustin, M. S.: Determinants of atmospheric mercury concentrations in Reno, Nevada, USA, Sci. Total Environ., 408, 431–438, 2009.

Lyman, S. N. and Jaffe, D. A.: Formation and fate of oxidized mercury in the upper troposphere and lower stratosphere, Nat. Geosci., 5, 114–117, doi:10.1038/NGEO1353, 2011.

Lyman, S. N., Jaffe, D. A., and Gustin, M. S.: Release of mercury halides from KCl denuders in the presence of ozone, Atmos. Chem. Phys., 10, 8197–8204, doi:10.5194/acp-10-8197-2010, 2010.

Lynam, M. M. and Keeler, G. J.: Automated speciated mercury measurements in Michigan, Environ. Sci. Technol., 39, 3289–3299, 2005.

Malcolm, E. G., Ford, A. C., Redding, T. A., Richardson, M. C., Strain, B. M., and Tetzner, S. W.: Experimental investigation of the scavenging of gaseous mercury by sea salt aerosol, J. Atmos. Chem., 63, 221–234, 2009.

Munthe, J., Wangberg, I., Iverfeldt, A., Lindqvist, O., Stromberg, D., Sommar, J., Gårdfeldt, K., Petersen, G., Ebinghaus, R., Prestbo, E., Larjava, K., and Siemens, V.: Distribution of atmospheric mercury species in Northern Europe: final results from the MOE project, Atmos. Environ., 37, 9–20, 2003.

Murphy, D. M., Hudson P. K., Thompson, D. S., Sheridan, P. J., and Wilson, J. C.: Observations of mercury-containing aerosols, Environ. Sci. Technol., 40, 3163–3167, 2006.

Two new sources of reactive gaseous mercury in the free troposphere

H. Timonen et al.

Title Page

Abstract | Introduction

Conclusions | References

Tables | Figures

◄ | ►

Back | Close

Full Screen / Esc

Printer-friendly Version

Interactive Discussion

NRC: Global Sources of Local Pollution: an Assessment of Long-Range Transport of Key Air Pollutants to and from the United States, The National Academies Press, Washington, DC, USA, 2010.

Obrist, D., Tas, E., Peleg, M., Matveev, V., Faïn, X., Asaf, D., and Luria, M.: Bromine-induced oxidation of mercury in the mid-latitude atmosphere, Nat. Geosci., 4, 22–26, 2010.

Pacyna, E. G., Pacyna, J. M., Sundseth, K., Munthe, J., Kindbom, K., Wilson, S., Steenhuisen, F., and Maxson, P.: Global emission of mercury to the atmosphere from anthropogenic sources in 2005 and projections to 2020, Atmos. Environ., 44, 2487–2499, 2010.

Pankow, J. F.: An absorption-model of the gas aerosol partitioning involved in the formation of secondary organic aerosol, Atmos. Environ., 28, 189–193, doi:10.1016/1352-2310(94)90094-9, 1994.

Parrella, J. P., Jacob, D. J., Liang, Q., Zhang, Y., Mickley, L. J., Miller, B., Evans, M. J., Yang, X., Pyle, J. A., Theys, N., and Van Roozendael, M.: Tropospheric bromine chemistry: implications for present and pre-industrial ozone and mercury, Atmos. Chem. Phys., 12, 6723–6740, doi:10.5194/acp-12-6723-2012, 2012.

Perry, K. D., Cliff, S. S., and Jimenez-Cruz, M. P.: Evidence for hygroscopic mineral dust particles from the Intercontinental Transport and Chemical Transformation Experiment, J. Geophys. Res., 109, D23S28, doi:10.1029/2004JD004979, 2004.

Peterson, C., Gustin, M., and Lyman, S.: Atmospheric mercury concentrations and speciation measured from 2004 to 2007 in Reno, Nevada, USA, Atmos. Environ., 43, 4646–4654, 2009.

Price, H. U., Jaffe, D. A., Cooper, O. R., and Doskey, P. V.: Photochemistry, ozone production, and dilution during long-range transport episodes from Eurasia to the Northwest United States, J. Geophys. Res., 109, D23S13, doi:10.1029/2003JD004400, 2004.

Raabe, O. G., Braaten, D. A., Axelbaum, R. L., Teague, S. V., and Cahill, T. A.: Calibration studies of the DRUM impactor, J. Aerosol Sci., 19, 183–195, 1988.

Rothenberg, S. E., McKee, L., Gilbreath, A., Yee, D., Connor, M., and Fu, X.: Evidence for short-range transport of atmospheric mercury to a rural, inland site, Atmos. Environ., 44, 1263–1273, doi:10.1016/j.atmosenv.2009.12.032, 2009.

Rutter, A. P. and Schauer, J. J.: The impact of aerosol composition on the particle to gas partitioning of reactive mercury, Environ. Sci. Technol., 41, 3934–3939, doi:10.1021/es062439i, 2007a.

Rutter, A. P. and Schauer, J. J.: The effect of temperature on the gas-particle partitioning of reactive mercury in atmospheric aerosols, Atmos. Environ., 41, 8647–8657, doi:10.1016/j.atmosenv.2007.07.024, 2007b.

Rutter, A. P., Shakya, K. M., Lehr, R., Schauer, J. J., and Griffin, R. J.: Oxidation of gaseous elemental mercury in the presence of secondary organic aerosols, Atmos. Environ., 59, 86–92, 2012.

Schroeder, W. H. and Munthe, J.: Atmospheric mercury – an overview, Atmos. Environ., 32, 809–822, 1998.

Selin, N. E., Jacob, D. J., Park, R. J., Yantosca, R. M., Strode, S., Jaegle, L., and Jaffe, D.: Chemical cycling and deposition of atmospheric mercury: global constraints from observations, J. Geophys. Res., 112, D02308, doi:10.1029/2006JD007450, 2007.

Sigler, J. M., Mao, H., and Talbot, R.: Gaseous elemental and reactive mercury in Southern New Hampshire, Atmos. Chem. Phys., 9, 1929–1942, doi:10.5194/acp-9-1929-2009, 2009.

Sillman, S., Marsik, F. J., Al-Wali, K. I., Keeler, G. J., and Landis, M. S.: Reactive mercury in the troposphere: model formation and results for Florida, the Northeastern United States, and the Atlantic Ocean, J. Geophys. Res., 112, D23305, doi:10.1029/2006JD008227, 2007.

Spivakovski, C. M., Logan, J. A., Montzka, S. A., Blkanski, Y. J., Foreman-Fowler, M., Jones, D. B. A., Horowitz, L. W., Fusco, A. C., Brenninkmeijer, C. A. M., Prather, M. J., Wofsy, S. C., and McElroy, M. B.: Three-dimensional climatological distribution of tropospheric OH: update and evaluation, J. Geophys. Res., 105, 8931–8980, 2000.

Sprovieri, F., Pirrone, N., Ebinghaus, R., Kock, H., and Dommergue, A.: A review of worldwide atmospheric mercury measurements, Atmos. Chem. Phys., 10, 8245–8265, doi:10.5194/acp-10-8245-2010, 2010.

Stephens, C. R., Shepson, P. B., Steffen, A., Bottenheim, J. W., Liao, J., Huey, L. G., Apel, E., Weinheimer, A., Hall, S. R., Cantrell, C., Sive, B. C., Knapp, D. J., Montzka, D. D., and Hornbrook, R. S.: The relative importance of chlorine and bromine radicals in the oxidation of atmospheric mercury at Barrow, Alaska, J. Geophys. Res., 117, D00R11, doi:10.1029/2011JD016649, 2012.

Subir, M., Ariya, P. A., and Dastoor, A. P.: A review of uncertainties in atmospheric modeling of mercury chemistry I. Uncertainties in existing kinetic parameters – fundamental limitations and the importance of heterogeneous chemistry, Atmos. Environ., 45, 5664–5676, 2011.

Subir, M., Ariya, P. A., and Dastoor, A. P.: A review of the sources of uncertainties in atmospheric modeling II. Mercury surface and heterogeneous chemistry – a missing link, Atmos. Environ., 46, 1–10, 2012.

Swartzendruber, P. C., Jaffe, D. A., Prestbo, E. M., Weiss-Penzias, P., Selin, N. E., Park, R., Jacob, D. J., Strode, S., and Jaeglé, L.: Observations of reactive gaseous mercury in the free troposphere at the Mount Bachelor Observatory, J. Geophys. Res., 111, D24301, doi:10.1029/2006JD007415, 2006.

Swartzendruber, P. C., Chand, D., Jaffe, D. A., Smith, J., Reidmiller, D., Gratz, L., Keeler, J., Strode, S., Jaeglé, L., and Talbot, R.: Vertical distribution of mercury, CO, ozone, and aerosol scattering in the Pacific Northwest during the spring 2006 INTEX-B campaign, J. Geophys. Res., 113, D10305, doi:10.1029/2007JD009579, 2008.

Talbot, R., Mao, H., Scheuer, E., Dibb, J., and Avery, M.: Total depletion of Hg^0 in the upper troposphere-lower stratosphere, Geophys. Res. Lett., 34, L23804, doi:10.1029/2007GL031366, 2007.

Talbot, R., Mao, H., Scheuer, E., Dibb, J., Avery, M., Browell, E., Sachse, G., Vay, S., Blake, D., Huey, G., and Fuelberg, H.: Factors influencing the large-scale distribution of Hg^0 in the Mexico City area and over the North Pacific, Atmos. Chem. Phys., 8, 2103–2114, doi:10.5194/acp-8-2103-2008, 2008.

Tas, E., Obrist, D., Peleg, M., Matveev, V., Faïn, X., Asaf, D., and Luria, M.: Measurement-based modelling of bromine-induced oxidation of mercury above the Dead Sea, Atmos. Chem. Phys., 12, 2429–2440, doi:10.5194/acp-12-2429-2012, 2012.

Thornton, J. A., Kercher, J. P., Riedel, T. P., Wagner, N. L., Cozic, J., Holloway, J. S., Dube, W. P., Wolfe, G. M., Quinn, P. K., Middlebrook, A. M., Alexander, B., and Brown, S. S.: A large atomic chlorine source inferred from mid-continental reactive nitrogen chemistry, Nat. Geosci., 464, 271–274, doi:10.1038/nature08905, 2009.

Weiss-Penzias, P., Jaffe, D. A., McClintick, A., Prestbo, E. M., and Landis, M. S.: Gaseous elemental mercury in the marine boundary layer: evidence for rapid removal in anthropogenic pollution, Environ. Sci. Technol., 37, 3755–3763, 2003.

Weiss-Penzias, P., Jaffe, D. A., Swartzendruber, P., Dennison, J. B., Chand, D., Hafner, W., and Prestbo, E.: Observations of Asian air pollution in the free troposphere at Mount Bachelor Observatory during the spring of 2004, J. Geophys. Res., 111, D10304, doi:10.1029/2005JD006522, 2006.

Weiss-Penzias, P., Jaffe, D., Swartzendruber, P., Hafner, W., Chand, D., and Prestbo, E.: Quantifying Asian and biomass burning sources of mercury using the Hg/CO ratio in pollution plumes observed at the Mount Bachelor observatory, Atmos. Environ., 41, 4366–4379, 2007.

Weiss-Penzias, P., Gustin, M. S., and Lyman, S. N.: Observations of speciated atmospheric mercury at three sites in Nevada: evidence for a free tropospheric source of reactive gaseous mercury, J. Geophys. Res., 114, D14302, doi:10.1029/2008JD011607, 2009.

Xiu, G., Cai, J., Zhang, W., Zhang, D., Büeler, A., Lee, S., Shen, Y., Xu, L., Huang, X., and Zhang, P.: Speciated mercury in size-fractionated particles in Shanghai ambient air, Atmos. Environ., 43, 3145–3154, 2009.

Two new sources of reactive gaseous mercury in the free troposphere

H. Timonen et al.

Table 1. Chemical characteristics of ALRT (type 2) and MBL (type 3) high-RGM events observed at MBO.

Event time period (UTC)[a]	Max RGM (pg m^{-3})	Avg. GEM (ng m^{-3})	Avg. THg (ng m^{-3})	Max RGM/GEM (%)	Max CO (ppbv)	Max O$_3$ (ppbv)	Max σ_{sp} (Mm^{-1})	R[b] (RGM vs. GEM)	R[b] (σ_{sp} vs. RGM)	R[b] (CO vs. RGM)	R[b] (σ_{sp} vs. CO)
ALRT											
16 Apr 17:00–18 Apr 14:00, 2008[c]	255	1.61 ± 0.07	1.73 ± 0.08	16	164	71	23.4	−0.67*	0.67*	−0.54	0.35
12 May 07:00–13 May 03:00, 2006	235	1.68 ± 0.09	1.80 ± 0.04	15	153	69	19.5	−0.77	0.94**	0.53	0.75
28 Apr 00:00–29 Apr 21:00, 2007[d]	290	1.65 ± 0.10	1.80 ± 0.08	18	157	77	9.5	−0.68*	0.32	0.60*	0.79**
MBL											
8 May 22:00–10 May 15:00, 2007	706	0.91 ± 0.28	1.40 ± 0.05	105	89	42	1.9	−0.97**	−0.76**	−0.82**	0.88**
21 Jun, 2007, 01:00–21:00	547	0.89 ± 0.10	1.37 ± 0.03	67	63	23	1	−0.92*	−0.81	−0.78	0.98**
7 Jul 11:00–10 Jul 04:00, 2007	388	1.25 ± 0.14	1.39 ± 0.09	40	82	43	1.7	−0.81*	−0.37	−0.61*	0.90**
10 May 01:00–12 May 01:00, 2011	275	1.12 ± 0.25	1.27 ± 0.12	31	90	42	1.5	−0.92**	−0.34	−0.79**	0.06

[a] The event time period includes the maximum RGM enhancement and up to 14 h preceding and following a discernible increase in RGM associated with the peak enhancement. Correlation parameters were calculated for this time period ($n = 5$–15), while the mean and maximum values for each listed chemical parameter correspond with only the times for which RGM was > 10 % of Max RGM ($n = 2$–6).

[b] Pearson correlation coefficient; *: $p < 0.05$; **: $p < 0.01$; no star: $p > 0.05$.

[c] Some CO data are missing for this event, which would tend to reduce the statistical significance of correlations between CO and other parameters. The R values corresponding with CO are likely not fully representative of the relationships to other measured parameters during this event.

[d] One 3-h averaged measurement (04:00 UTC on 29 April) with a possible UT/LS influence was excluded when calculating the values presented here.

Table 2. Conditions specified in the box model of RGM production via Br-initiated Hg^0 oxidation. Conditions common to all scenarios: $T = 281.9\,K$; $P = 896.4\,hPa$; $[GEM]_0 = 1.194\,ng\,m^{-3}$; $[HgBr]_0 = [RGM]_0 = 0$; RGM = HgBr + HgBrX, where X = Br, OH.

Parameter	Model Scenario			
	Low_Br_low_HO	High_Br_low_HO	Low_Br_high_HO	High_Br_high_HO
$[Br^\bullet]_{average}$ (pptv)	0.010	0.035	0.010	0.035
$[Br^\bullet]_{max}$ (pptv)	0.020	0.072	0.020	0.072
$[HO^\bullet]_{average}$ (pptv)	0.021	0.021	0.063	0.063
$[HO^\bullet]_{max}$ (pptv)	0.043	0.043	0.13	0.13
$[GEM]_{final}$ ($ng\,m^{-3}$)	1.165	1.052	1.149	1.019
$[HgBr]_{max}$ ($pg\,m^{-3}$)	0.26	0.66	0.20	0.54
$[RGM]_{final}$ ($pg\,m^{-3}$)	29	142	45	175

Diel variability in $[Br^\bullet]$ and $[HO^\bullet]$ was approximated with sinusoidal functions having periods of 24 h. The $[HO^\bullet]$ diel peak was delayed by 4 h compared with that of $[Br^\bullet]$ to approximate the expected relationship between the diel cycles of these radicals in the MBL (Holmes et al., 2010; Goodsite et al., 2004). The range of average $[Br^\bullet]$ is from Holmes et al. (2009) (for the Pacific MBL) and from Parrella et al. (2012) (annual zonal mean, corresponding approximately with the latitude and altitude of the MBO observations). The range of average $[HO^\bullet]$ is from Spivakovski et al. (2000), corresponding approximately with the latitude, altitude, and season of the MBO observations. The "final" concentrations are those attained after 10 days.

Two new sources of reactive gaseous mercury in the free troposphere

H. Timonen et al.
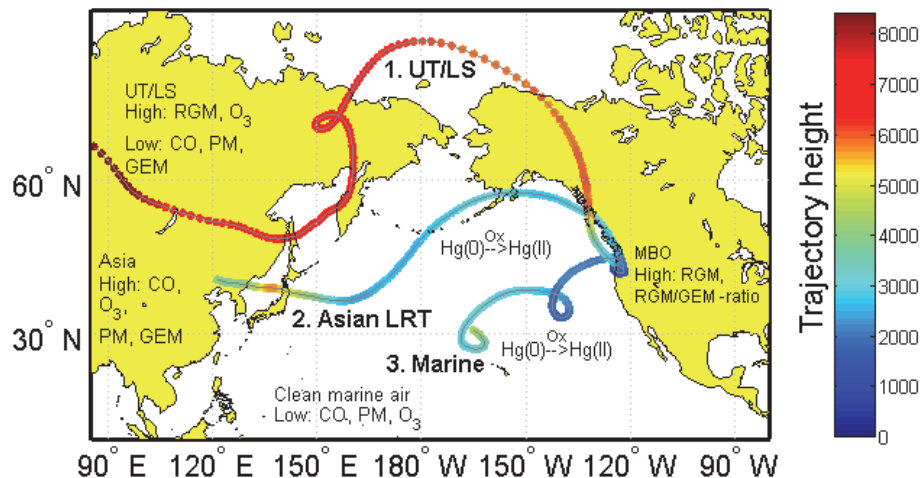
Fig. 1. Sources of RGM in the free troposphere as measured at MBO: 1, UT/LS (Swartzendruber et al., 2006; Ambrose et al., 2011) ; 2, ALRT (this paper); and 3, clean marine boundary layer (MBL) air masses processed in the FT above the Pacific Ocean (this paper). The HYSPLIT airmass back trajectories of three events (UT/LS: 22 April 2006; ALRT: 17 April 2008; MBL: 9 May 2007) are used to show a typical pathway of airmasses during each event type. Trajectories are colored by height. The typical chemical composition of airmasses (ozone (O_3), CO, and particulate matter (PM) concentrations) are shown for the areas where the trajectories originate. Key features of the Hg observations at MBO are also shown.
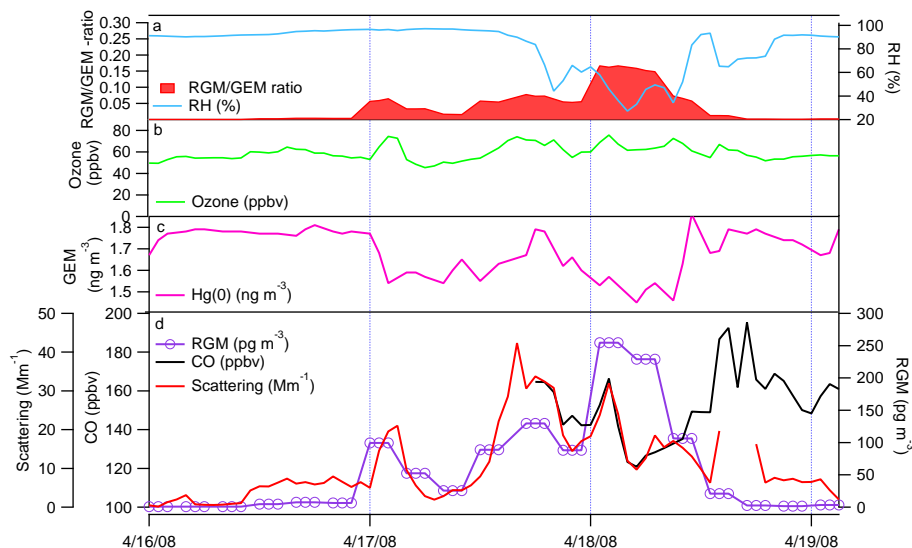
Fig. 2. Time series of **(a)** O_3 and relative humidity (RH); **(b)** RGM/GEM-ratio and GEM; **(c)** RGM, submicron aerosol scattering (σ_{sp}), and CO measured at MBO during a type 2 (ALRT) high-RGM event in spring 2008. All data are 1-h averages, except RGM and RGM/GEM-ratios that are 3-h averages (resolution of the RGM measurement). ($1\,\mathrm{ng\,m^{-3}} \approx 0.12$ parts per trillion by volume at 1.01 bar and 273 K.)
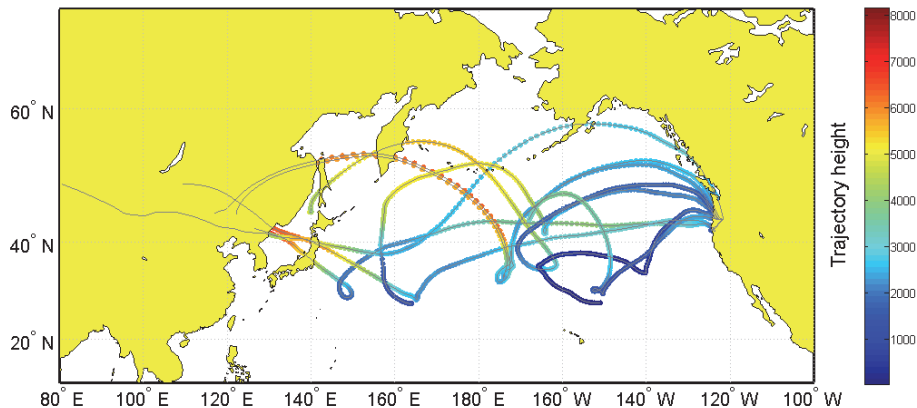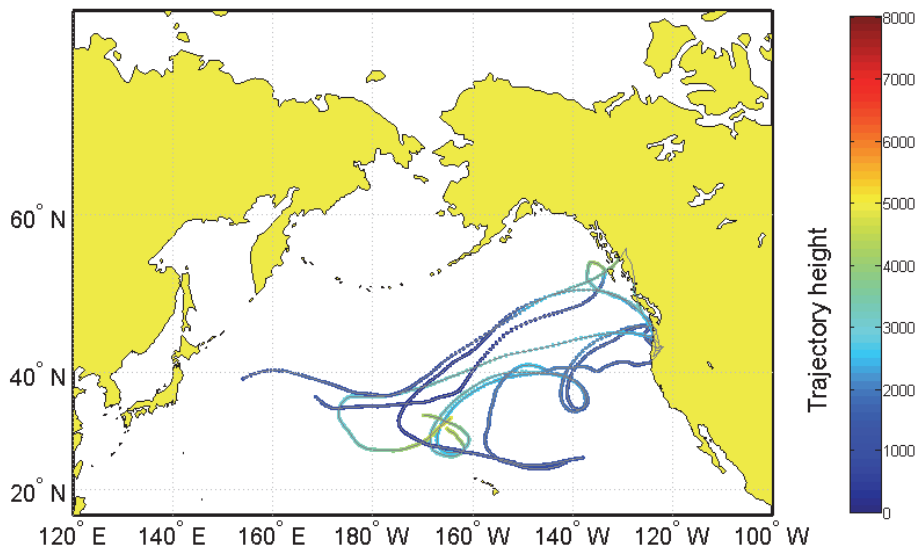
Fig. 3. Ten-day HYSPLIT airmass back trajectories for three Asian long-range transport (ALRT) high-RGM events. Trajectories were initialized at times during each event when the highest RGM/GEM-ratios were observed.

Back | Close

Full Screen / Esc

Printer-friendly Version

Interactive Discussion
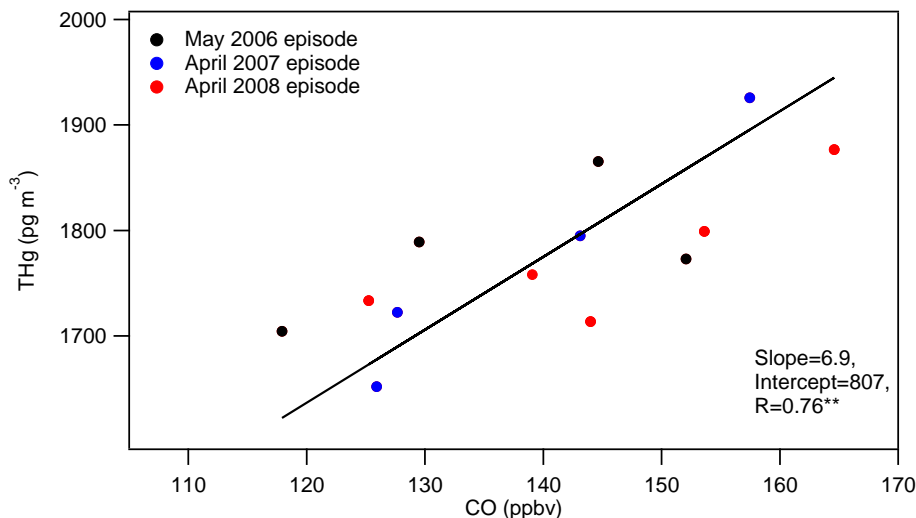
Fig. 4. Elevated CO and THg concentrations and THg/CO enhancement ratios measured during May 2006, April 2007, and April 2008 high-RGM events are suggestive of Asian long-range transport (ALRT). Due to the small number of data points during each individual event, we performed a linear regression analysis using all data combined. The THg/CO correlation slope for the combined events is similar to Asian emission ratios measured previously (Jaffe et al., 2005; Weiss-Penzias et al., 2007).
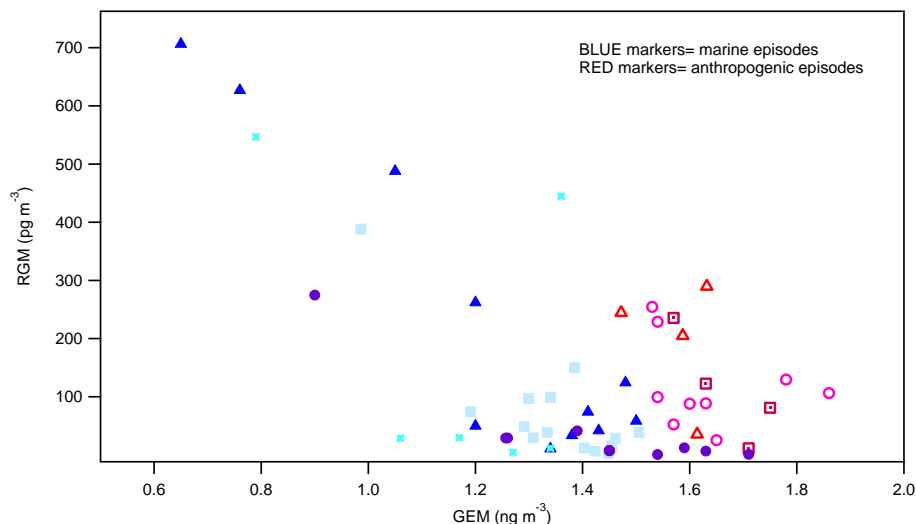
Fig. 5. A negative correlation was observed between RGM and GEM during high-RGM events. Elevated total mercury (THg) and RGM concentrations (peak values of 200–700 pg m^{-3}, elevated by up to ~0.2–0.7 ng m^{-3} and a factor of ~20–70 above typical background FT levels) were observed during MBL events. The GEM concentrations were higher during ALRT events (THg = 1.65–1.80 ng m^{-3}; 1 nanogram per cubic meter ≈ 0.12 parts per trillion by volume at 1.01 bar and 273 K). In general, the MBL events (type 3) show stronger inverse correlations between RGM and GEM compared to ALRT events (type 2).

Title Page

Abstract | Introduction

Conclusions | References

Tables | Figures

|◄ | ►|

◄ | ►

Back | Close

Full Screen / Esc

Printer-friendly Version

Interactive Discussion

Fig. 6. Ten-day HYSPLIT airmass back trajectories for the marine boundary layer (MBL) high-RGM events. Trajectories were initialized at times during each event when the highest RGM/GEM-ratios were observed.

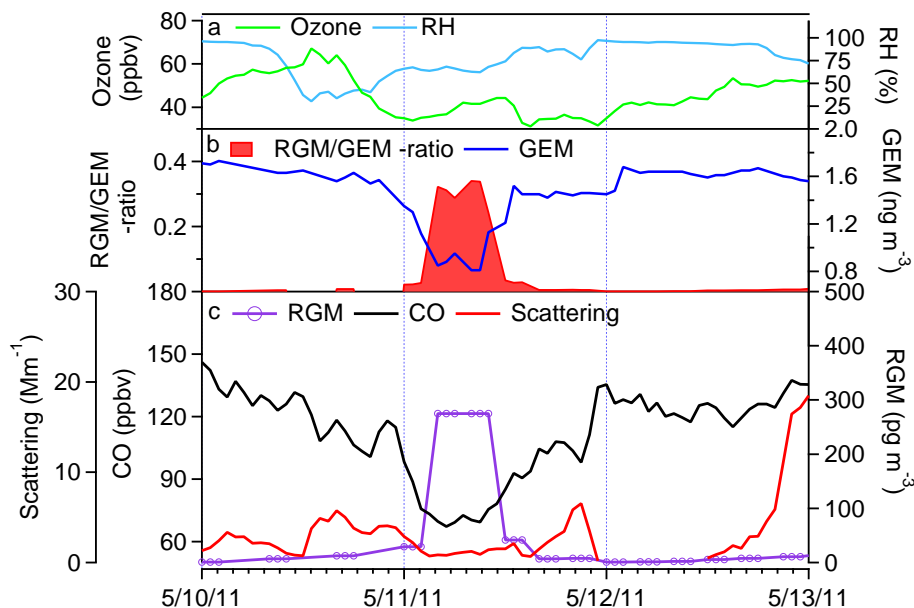**Fig. 7.** Time series of **(a)** O_3 and relative humidity (RH); **(b)** RGM/GEM-ratio and GEM; **(c)** RGM, submicron aerosol scattering (σ_{sp}), and CO measured at MBO during a type 3 (MBL) high-RGM event in spring 2011. All data are 1-h averages, except RGM and RGM/GEM-ratios that are 3-h averages (resolution of the RGM measurement).

Title Page

Abstract | Introduction

Conclusions | References

Tables | Figures

|◄ | ►|

◄ | ►

Back | Close

Full Screen / Esc

Printer-friendly Version

Interactive Discussion
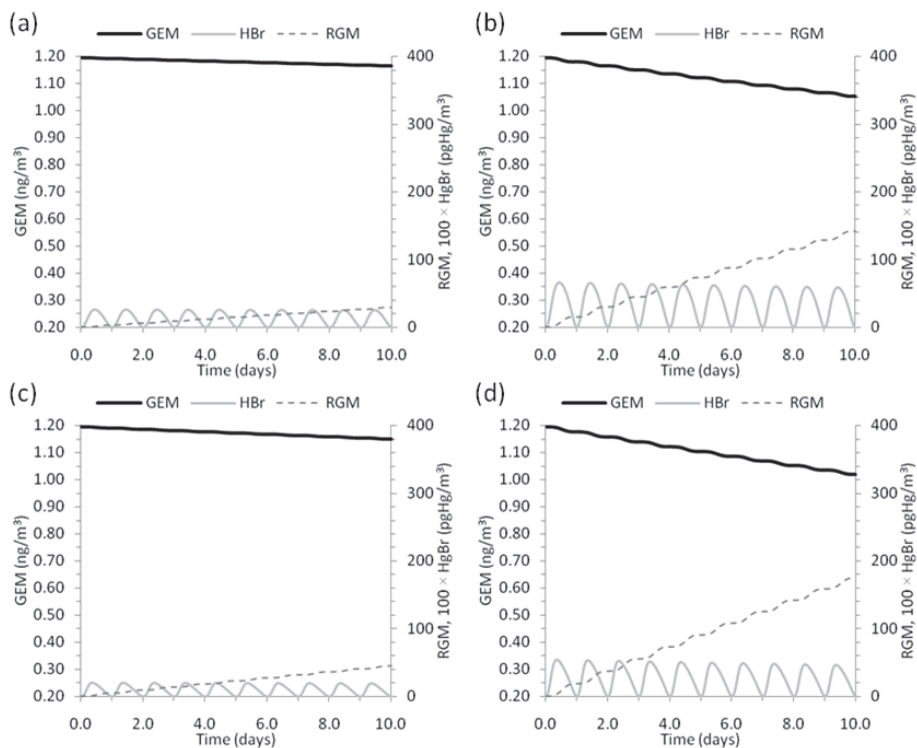
Fig. 8. Simulated Br-initiated oxidation of Hg^0 to RGM ($= HgBr + HgBrX$, where $X = Br$, OH) under conditions representative of the 11 May 2011 MBL high-RGM event. Model scenarios (defined in Table 2): **(a)** Low_Br_low_HO; **(b)** High_Br_low_HO; **(c)** Low_Br_high_HO ; **(d)** High_Br_high_HO.